2.2 Flexible rods

The various polymers and filaments in the cell display bending resistances whose numerical values span six orders of magnitude, from highly flexible alkanes through somewhat stiffer protein polymers such as F-actin, to moderately rigid microtubules. Viewed on micron length scales, these filaments may appear to be erratic, rambunctious chains or gently curved rods, and their elastic properties may be dominated by entropic or energetic effects. In selecting a formalism for interpreting the characteristics of cellular filaments, one can choose among several simple pictures of linear polymers, each picture emphasizing different aspects of the polymer. In this section, we view the filament as a smoothly curving rod, while in Sec. 2.3, our picture is that of a wiggly segmented chain. These two pictures of linear polymers overlap, of course, and there are links between their parametrizations.

Arc length and curvature

We first describe a rod as a continuous curve with no kinks or discontinuities, and ignore, for the time being, its cross-sectional shape and material composition. As displayed in Fig. 2.8(a), each point on the curve corresponds to a position vector $\mathbf{r}$, represented by the familiar Cartesian triplet (x, y, z). It is often convenient to write $\mathbf{r}$ and other characteristics of the curve in a parametric representation as a function of the arc length s, say $\mathbf{r}(s)$ or $[x(s), y(s), z(s)]$, where s follows along the contour of the curve, running from 0 at one end to the full contour length L_c at the other. As an illustration, the equation $x^2 + y^2 = R^2$ of a circle of radius R lying in the xy plane is represented in the parametric approach by $x(s) = R \cos(s/R)$ and $y(s) = R \sin(s/R)$, where the arc length s is zero at $(x,y) = (R,0)$.

The unit tangent vector $\mathbf{t}$ characterizes the direction of the curve as it winds its way through space, as shown in Fig. 2.8. For example, in two dimensions, $\mathbf{t}$ has (x,y) components $(\cos\theta, \sin\theta)$, where θ is the angle between $\mathbf{t}$ and the x-axis. For a short section of arc Δs, over which the curve appears straight, the pair $(\cos\theta, \sin\theta)$ can be

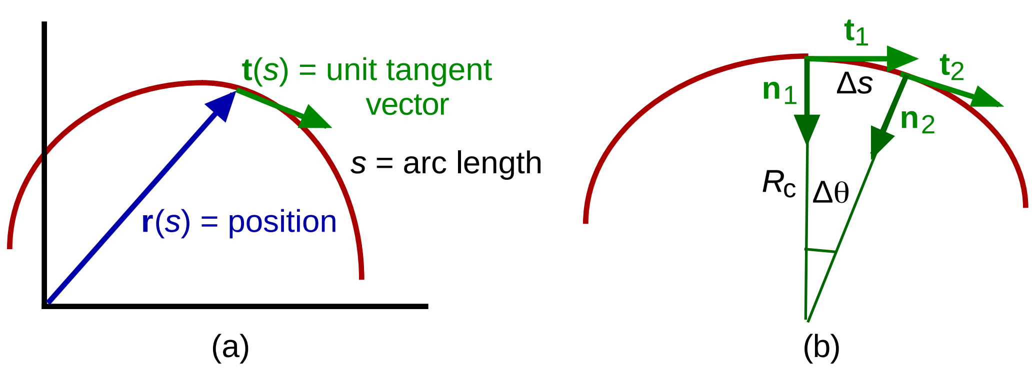

Fig. 2.8. (a) A point on the curve at arc length s is described by a position vector $\mathbf{r}(s)$ and a unit tangent vector $\mathbf{t}(s) = \partial\mathbf{r}/\partial s$. (b) Two locations are separated by an arc length Δs subtending an angle $\Delta\theta$ at a vertex formed by extensions of the unit normals $\mathbf{n}_1$ and $\mathbf{n}_2$. Extensions of $\mathbf{n}_1$ and $\mathbf{n}_2$ intersect at a distance R_c from the curve.

replaced by ($\Delta r_x/\Delta s$, $\Delta r_y/\Delta s$), which becomes ($\partial r_x/\partial s$, $\partial r_y/\partial s$) in the infinitesimal limit, or

$$\mathbf{t}(s) = \partial \mathbf{r}/\partial s, \tag{2.4}$$

a result valid in any number of dimensions. How does **t** change along the curve? Consider two nearby positions 1 and 2 on the curve illustrated in Fig. 2.8(b). If the curve were straight, the unit tangent vectors $\mathbf{t}_1$ and $\mathbf{t}_2$ at points 1 and 2 would be parallel; in other words, unit tangent vectors to a straight line are independent of position. However, such is not the case with curved lines, and the rate of change of **t** with *s* provides a measure of the curvature at any given position. As we recall from introductory mechanics, the vector $\Delta\mathbf{t} = \mathbf{t}_2 - \mathbf{t}_1$ is perpendicular to the curve in the limit where positions 1 and 2 are infinitesimally close. Thus, the rate of change of **t** with *s* is proportional to the unit normal to the curve **n**, and we define the proportionality constant to be the curvature *C*

$$\partial \mathbf{t}/\partial s = C\mathbf{n}, \tag{2.5}$$

where *C* has units of inverse length. We can substitute Eq. (2.4) into (2.5) to obtain

$$C\mathbf{n} = \partial^2 \mathbf{r}/\partial s^2. \tag{2.6}$$

The reciprocal of *C* is the local radius of curvature of the arc, which is displayed in Fig. 2.8(b) by extrapolating the unit normals $\mathbf{n}_1$ and $\mathbf{n}_2$ to their point of intersection. If positions 1 and 2 are close by on the contour, then the arc is approximately a segment of a circle with radius R_c and defines an angle $\Delta\theta = \Delta s / R_c$, where Δs is the segment length. However, $\Delta\theta$ is also the angle between $\mathbf{t}_1$ and $\mathbf{t}_2$; that is, $\Delta\theta = |\Delta\mathbf{t}| / t = |\Delta\mathbf{t}|$, the second equality following from $|\mathbf{t}| = t = 1$. Equating these two expressions for $\Delta\theta$ yields $|\Delta\mathbf{t}| / \Delta s = 1/R_c$, which can be compared with Eq. (2.5) to give

$$C = 1/R_c. \tag{2.7}$$

Lastly, the unit normal vector **n**, which is $\Delta\mathbf{t} / |\Delta\mathbf{t}|$, can be rewritten by using $|\Delta\mathbf{t}| = \Delta\theta$

$$\mathbf{n} = \partial \mathbf{t}/\partial\theta. \tag{2.8}$$

Bending energy of a thin rod

Suppose that we take a straight rod of length L_c with uniform density and cross section, and bend it into an arc with radius R_c, as in Fig. 2.6. The problem of finding the energy E_{arc} associated with this deformation is solved in many texts on continuum mechanics, and has the form (Landau and Lifshitz, 1986)

$$E_{arc} / L_c = \kappa_f / 2R_c^2 = Y\mathcal{I} / 2R_c^2, \tag{2.9}$$

where κ_f is called the flexural rigidity (units of [*energy*]•[*length*]), *Y* is the Young's modulus of the rod, and $\mathcal{I}$ is the moment of inertia of the cross section (see Fig. 2.9). The Young's modulus appears in expressions of the form [*stress*] = Y [*strain*], and has the same units as stress, since strain is dimensionless (see Appendix D for a review of elasticity theory). For three-dimensional materials, Y has units of energy density, and typically ranges from 10^9 J/m^3 for plastics to 10^{11} J/m^3 for metals.

The moment of inertia of the cross section is defined somewhat similarly to the moment of inertia of the mass: it is an area-weighted integral of the squared distance from an axis

$$\mathcal{I}_y = \int x^2 \, dA, \tag{2.10}$$

where the xy plane defined by the integration axes is perpendicular to the length of the rod, and dA is an element of surface area in that plane. For example, if the rod is a cylinder of radius R, the cross section has the shape of a solid disk with an area element dA at position x given by $dA = 2(R^2 - x^2)^{1/2} dx$, as shown in Fig. 2.9. Hence,

$$\mathcal{I}_y = 4 \int_0^R x^2 \, (R^2 - x^2)^{1/2} \, dx = \pi R^2/4 \quad \text{(solid cylinder).} \tag{2.11}$$

Should the rod have a hollow core of radius R_i, like a microtubule, then the moment of inertia in Eq. (2.11) would be reduced by the moment of inertia $\pi R_i^2/4$ of the core:

$$\mathcal{I}_y = \pi(R^4 - R_i^4)/4 \qquad \text{(hollow cylinder).} \tag{2.12}$$

Other rods of varying cross sectional shape are treated in the problem set.

The deformation energy per unit length of the arc in Eq. (2.9) is inversely proportional to the square of the radius of curvature, or, equivalently, is proportional to the square of the curvature C from Eq. (2.7). In fact, one would expect on general grounds that the leading order contribution to the energy per unit length must be C^2, just as the potential energy of an ideal spring is proportional to the square of the displacement from equilibrium. Alternatively, then, the energy per unit length could be written as $E_{arc}/L = \kappa_f \, (\partial \mathbf{t}/\partial s)^2/2$ by using Eq. (2.5). Further, there is no need for the curvature to be constant along the length of the filament, and the general expression

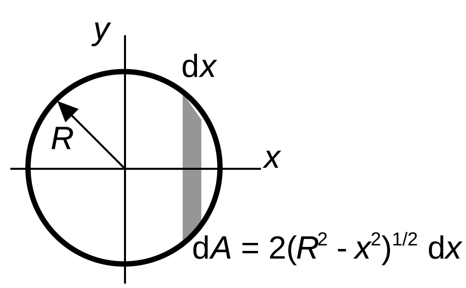

Fig. 2.9. Section through a cylindrical rod showing the xy axes used to evaluate the moment of inertia of the cross section $\mathcal{I}_y$ in Eq. (2.10).

for the total energy of deformation E_{bend} is, to lowest order,

$$E_{bend} = (\kappa_f/2) \int_0^{L_c} (\partial \mathbf{t}/\partial s)^2 \, ds, \tag{2.13}$$

where the integral runs along the length of the filament. This form for E_{bend} is called the Kratky-Porod model; it can be trivially modified to represent a rod with an unstressed configuration that is intrinsically curved.

Fluctuations and persistence length

At zero temperature, a filament adopts a shape that minimizes its energy, which corresponds to a straight rod if the energy is governed by Eq. (2.13). At non-zero temperature, the filament exchanges energy with its environment, permitting the shape to fluctuate, as illustrated in Fig. 2.10(a). According to Eq. (2.13), the bending energy of a filament rises as its shape becomes more contorted and the local curvature along the filament grows; hence, the bending energy of the configurations increases from left to right in Fig. 2.10(a). Now, the probability $\mathcal{P}(E)$ of the filament being found in a specific configuration with energy E is proportional to the Boltzmann factor $\exp(-\beta E)$, where β is the inverse temperature $\beta = 1/ k_B T$ (see Appendix C for a review). The Boltzmann factor tells us that the larger is the energy required to deform the filament into a specific shape, the lower is the probability that the filament will have that shape, all other things being equal. Thus, a filament will adopt configurations with small average curvature if their flexural rigidity is high or the temperature is low; their shape will resemble sections of circles, becoming contorted only at high temperatures.

Let us assume that our filament can sustain only gentle curves and has constant curvature; neither is our filament so long that it closes upon itself. The shape can then be uniquely parametrized by the angle θ between the unit tangent vectors $\mathbf{t}(0)$ and $\mathbf{t}(s)$ at the two ends of the filament [see Fig. 2.10(b)] and has a specific energy E_{bend} given by Eq. (2.9). For an arc of a circle with radius R_c, the angle θ is the same as that

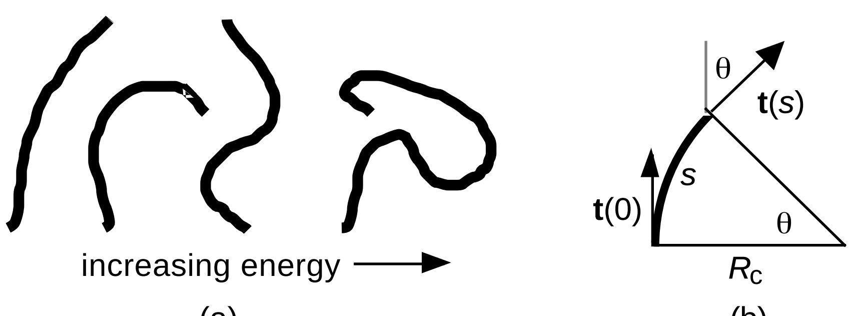

Fig. 2.10. (a) Sample of configurations available to a filament; for a given κ_f the bending energy of the filament rises as its shape becomes more contorted. (b) If the filament is a section of a circle, the angle subtended by the arc length s is the same as the change in the direction of the unit tangent vector $\mathbf{t}$ along the arc.

subtended by the arc of length s (that is, $\theta = s / R_c$) such that Eq. (2.9) can be written as

$$E_{arc} = \kappa_f s / 2R^2 = \kappa_f \theta^2 / 2s. \qquad (2.14)$$

For now, we use s to denote the length of filament, rather than L_c, since the result that we are about to obtain also applies to short segments of more sinuous filaments, just as long as the segment has constant curvature.

The angle θ changes as the filament waves back and forth: at higher temperatures, the oscillations have a larger amplitude and the filament samples larger values of θ than at lower temperatures. To characterize the magnitude of the oscillations, we evaluate the mean value of θ^2, denoted by the conventional $\langle\theta^2\rangle$. If the filament has a constant length, $\langle\theta^2\rangle$ involves a weighted average of the three-dimensional position sampled by the end of the filament. That is, with one end of the filament defining the direction of a coordinate axis (say the z-axis), the other end is described by the polar angle θ and the azimuthal angle ϕ. Assuming that the shapes in the ensemble are arcs of circles, the probability of each configuration is equal to $\wp(E_{arc})$, so that

$$\langle\theta^2\rangle = \int \theta^2 \wp(E_{arc}) \mathrm{d}\Omega \; / \int \wp(E_{arc}) \mathrm{d}\Omega, \qquad (2.15)$$

where the integral must be performed over the solid angle $\mathrm{d}\Omega = \sin\theta \; d\theta \; \mathrm{d}\phi$. The bending energy E_{arc} is independent of ϕ, allowing the azimuthal angle to be integrated out, leaving

$$\langle\theta^2\rangle = \int \theta^2 \exp(-\beta E_{arc}) \sin\theta \, \mathrm{d}\theta \; / \int \exp(-\beta E_{arc}) \sin\theta \, \mathrm{d}\theta, \qquad (2.16)$$

where the minimum value of θ in the integrals is 0, and $\wp(E_{arc})$ has been replaced by the Boltzmann factor.

By assumption, our filaments are sufficiently stiff that E_{arc} increases rapidly with θ; that is, we consider only small oscillations in the filament shape. As a consequence, the Boltzmann factor decays rapidly with θ, meaning that $\sin\theta$ is sampled only at small θ, and can be replaced by the small angle approximation $\sin\theta \sim \theta$. Hence, Eq. (2.16) becomes

$$\langle\theta^2\rangle = (2s / \beta\kappa_f) \int x^3 \exp(-x^2) \, \mathrm{d}x \; / \int x \exp(-x^2) \, \mathrm{d}x, \qquad (2.17)$$

after substituting Eq. (2.14) for E_{arc} and changing variables to $x = (\beta\kappa_f / 2s)^{1/2}\theta$. In the small oscillation approximation, the upper limits of the integrals in Eq. (2.17) can be extended to infinity with little error, whence both integrals are equal to 1/2 and cancel.

Thus, the expression for the mean square value of θ is

$$\langle \theta^2 \rangle \quad 2s / \beta\kappa_f \qquad \text{(small oscillations).} \tag{2.18}$$

The combination $\beta\kappa_f$ has the units of length, and is defined as the persistence length ξ_p of the filament:

$$\xi_p \equiv \beta\kappa_f. \tag{2.19}$$

Note that the persistence length decreases with increasing temperature.

The variation in the direction of the tangent vectors provides a geometrical interpretation of the persistence length. Consider the scalar product of the unit tangent vectors $\mathbf{t}(0)\bullet\mathbf{t}(s)$, which has its maximum value of unity only if the tangent vectors are parallel at the ends of the filament. At non-zero temperature, the filament samples a variety of orientations such that the ensemble average $\langle\mathbf{t}(0)\bullet\mathbf{t}(s)\rangle = \langle\cos\theta\rangle$ has a maximum absolute value of unity. The quantity $\langle\mathbf{t}(0)\bullet\mathbf{t}(s)\rangle$ is referred to as the correlation function of the tangent vector: it describes the correlation between the direction of the tangent vectors at different positions along the curve. At low temperatures where θ is usually small, $\cos\theta$ can be approximated by $\cos\theta \sim 1 - \theta^2/2$, permitting the correlation function to be written as

$$\langle\mathbf{t}(0)\bullet\mathbf{t}(s)\rangle \sim 1 - \langle\theta^2\rangle/2. \tag{2.20}$$

The dispersion in θ in this small oscillation limit is given by Eq. (2.18), so that

$$\langle\mathbf{t}(0)\bullet\mathbf{t}(s)\rangle \sim 1 - s/\xi_p \qquad (s/\xi_p \ll 1), \tag{2.21}$$

which can be used to obtain the mean squared difference in the tangent vectors

$$\langle [\mathbf{t}(s) - \mathbf{t}(0)]^2 \rangle = 2 - 2\langle\mathbf{t}(0)\bullet\mathbf{t}(s)\rangle \sim 2s/\xi_p \qquad (s/\xi_p \ll 1). \tag{2.22}$$

Thus, the persistence length measures the distance along the filament over which the orientation of the curve becomes decorrelated.

For a rigid rod, meaning a rod whose contour length L_c is short compared to ξ_p, Eq. (2.21) correctly predicts that $\langle\mathbf{t}(0)\bullet\mathbf{t}(L_c)\rangle \sim 1$, and also correctly predicts that the correlations initially die off linearly as contour length grows. However, if $L_c \gg \xi_p$, the filament appears floppy and $\langle\mathbf{t}(0)\bullet\mathbf{t}(L_c)\rangle$ should vanish as the tangent vectors at the extreme ends of the filament become uncorrelated, a behavior not seen in Eq. (2.21) because it was derived in the limit of small oscillations. Rather, the correct expression for the tangent correlation function applicable at short and long distances is

$$\langle\mathbf{t}(0)\bullet\mathbf{t}(s)\rangle = \exp(-s/\xi_p), \tag{2.23}$$

from which we see that Eq. (2.21) is the leading order approximation *via* $\exp(-x) \sim 1-x$ at small x. Intuitively, one would expect to obtain an expression like Eq. (2.23) by applying Eq. (2.21) repeatedly to successive sections of the filament; a more detailed derivation can be found in Doi and Edwards (1986).